Environ. Sci. Technol. **2010,** *44,* 184–190

Bioreduction of Nitrobenzene, Natural Organic Matter, and Hematite by *Shewanella putrefaciens* CN32

FUBO LUAN,[†,‡] WILLIAM D. BURGOS,*[,†] LI XIE,[‡] AND QI ZHOU[‡]

Department of Civil and Environmental Engineering, The Pennsylvania State University, University Park, Pennsylvania, and State Key Laboratory of Pollution Control and Resources Reuse, School of Environmental Science and Engineering, Tongji University, 1239 Siping Road, Shanghai 200092, China

Received June 4, 2009. Revised manuscript received October 31, 2009. Accepted November 3, 2009.

We examined the reduction of nitrobenzene by *Shewanella putrefaciens* CN32 in the presence of natural organic matter (NOM) and hematite. Bioreduction experiments were conducted with combinations and varied concentrations of nitrobenzene, soil humic acid, Georgetown NOM, hematite, and CN32. Abiotic experiments were conducted to quantify nitrobenzene reduction by biogenic Fe(II) and by bioreduced NOMs. We show that *S. putrefaciens* CN32 can directly reduce nitrobenzene. Both NOMs enhanced nitrobenzene reduction and the degree of enhancement depended on properties of the NOMs (aromaticity, organic radical content). Hematite enhanced nitrobenzene reduction by indirect reaction with biogenic-Fe(II), however, enhancement was dependent on the availability of excess electron donor. Under electron donor-limiting conditions, reducing equivalents diverted to hematite were not all transferred to nitrobenzene. In systems that contained both NOM and hematite we conclude that NOM-mediated reduction of nitrobenzene was more important than Fe(II)-mediated reduction.

Introduction

Soil and groundwater contamination caused by the production and storage of explosives and ammunition is a significant problem for military facilities. Organic contaminants associated with explosives include trinitrotoluene (TNT) and hexahydro-1,3,5-trinitro-1,3,5-triazine (RDX). Because of its relatively simple structure, we have chosen nitrobenzene as a model nitroaromatic compound (NAC) to study the multiple pathways operative for NAC reduction under iron(III)-reducing conditions (Figure 1). In anoxic subsurface environments, the presence of dissimilatory metal-reducing bacteria (DMRB) and natural organic matter (NOM) significantly contribute to the complexity of this biogeochemical system.

The "direct" biological reduction of nitro-compounds by pure bacterial cultures has been reported for several DMRB, including *Geobacter metallireducens*, *G. sulfurreducens*, *Anaeromyxobacter dehalogenans*, *Shewanella oneidensis* MR-1, and *Desulfitobacterium chlororespirans* with cyclic nitramines (*1*−*3*); *Clostridium* sp. EDB2 with cyclic nitramines (*4*); *Cellulomonas* sp. ES6 with TNT (*5*); *G. metallireducens* with chloro-substituted nitrobenzenes (*6*−*8*); and *S. putrefaciens* CN32 with 4-cyano-4′-aminoazobenzene (CNAAzB) (*9*). The results from these studies have been variable with respect to the DMRB's ability to respire on the various nitro-compounds. The fermentative bacteria such as *Cellulomonas* and *Clostridium* were able to respire on TNT (*5*) and RDX (*4*), respectively, and subsequently promote further biodegradation beyond the initial nitro-reduction step. While *G. metallireducens* could reduce RDX (*1*), it could not directly reduce 4-nitroacetophenone (*8*) or 4-chloronitrobenzene (*6, 7*). *S. oneidensis* MR-1 could reduce RDX, albeit at extremely slow rates (*2*), while *S. putrefaciens* CN32 could not reduce CNAAzB (*9*).

When iron(III) (hydr)oxides are added to systems containing DMRB and NACs, Fe(III) reduction may compete with NAC reduction for available electron donor, and/or produce biogenic Fe(II) that serves as a reductant of the NAC. The effect of solid-phase Fe(III) on NAC (bio)reduction has, in turn, been variable. For example, the addition of ferrihydrite to suspensions of *G. metallireducens* with RDX decreased the contaminant decay rate (*1, 2*), while the addition of ferrihydrite was required for *G. metallireducens* to reduce 4-nitroacetophenone (*8*) or 4-chloronitrobenzene (*6*). When NOM is added to systems containing DMRB, NACs, and Fe(III) it is presumed to act as a catalytic electron shuttle and enhance the reduction of both solid-phase Fe(III) (*10*−*14*) and soluble NACs (*1*). However, because NOM can sorb to Fe(III) surfaces it can also interfere with electron transfer reactions between the NACs and solid-associated Fe(II) (*15, 16*).

Reaction pathways of NACs in natural environments that contain DMRB, solid Fe(III), and NOM are difficult to generalize. The current literature suggests that characteristics of the DMRB (i.e., metabolic capabilities), iron mineral (e.g., crystallinity, surface area), NOM (e.g., quinone content, hydrophobicity), and NAC (i.e., chemical structure, reduction potential) will all exert an effect on NAC transformations. Therefore, the objective of this research was to use model systems containing nitrobenzene with varied combinations of *S. putrefaciens* CN32, hematite, and humic substances to better quantify biotic and abiotic contaminant transformations.

Experimental Section

Microorganism and Culture Conditions. *Shewanella putrefaciens* strain CN32 (hereafter referred to as CN32) was grown aerobically on tryptic soy broth without dextrose (Difco) at 20 °C, and cells were harvested and prepared anaerobically as previously described (*12, 17*).

Chemicals and Minerals. Reagent grade nitrobenzene and aniline (Fluka) were used to prepare 0.16 M stock solutions in methanol. Hematite (Fisher) was used to prepare a 2 g L^{-1} stock solution in deoxygenated 10 mM PIPES buffer (pH 6.8). Two NOMs were used in these experiments: soil humic acid (SHA) purchased from the International Humic Substances Society (IHSS), and Georgetown NOM (GNOM) (*18*) provided courtesy of Dr. Baohua Gu (Oak Ridge National Laboratory). SHA and GNOM were used to prepare 1 g L^{-1} stock solutions in deoxygenated 10 mM PIPES buffer (pH 6.8).

Biotic Experiments. All experiments were conducted in 160-mL serum bottles crimp-sealed with Teflon-faced rubber stoppers. All preparations were performed in an anaerobic chamber (Coy, Grass Lakes, MI) under a N_2:H_2 atmosphere

* Corresponding author phone: 814-863-0578; fax: 814-863-7304; e-mail: wdb3@psu.edu.
[†] The Pennsylvania State University.
[‡] Tongji University.

10.1021/es901585z

Published on Web 12/03/2009

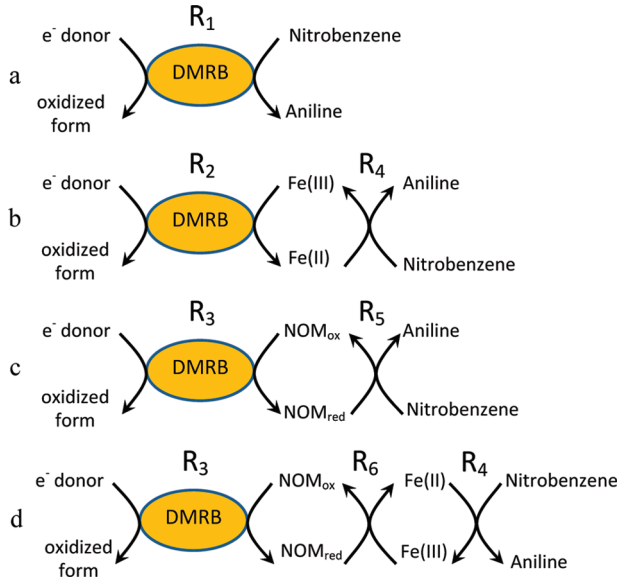

FIGURE 1. Proposed pathways for the enhancement of nitrobenzene (NB) reduction in systems containing DMRB, Fe(III) oxides, and NOM. Reaction numbers R_1–R_6 correspond to discussions in the text and Tables 1 and 2. (a) Direct bioreduction of NB; (b) indirect reduction of NB by biogenic Fe(II); (c) indirect reduction of NB by bioreduced NOM; and (d) indirect reduction of NB coupled to both NOM and Fe(III) reduction.

(97.5:2.5%) at room temperature. Reactors were filled with ca. 100 mL of deoxygenated 10 mM PIPES buffer (pH 6.8) containing various combinations of nitrobenzene (149 or 1490 μM), CN32 (0 or 1 × 10^8 cell mL^{-1}), NOM (10 or 100 mg L^{-1}), and hematite (0.2 or 2.0 g L^{-1}) (Table 1). H_2 in the reactor headspace (2.5%) served as the electron donor. Lactate (5 mM) was provided in select experiments. Reactors were incubated at 100 rpm on orbital shakers within the anaerobic chamber. A series of control reactors were prepared with every experiment: abiotic controls that were not inoculated with CN32, and biotic controls that contained no NOM, hematite, or nitrobenzene. All treatments and controls were run in triplicate. After cell inoculation, samples were periodically removed with sterile needle and syringe (in chamber) and nitrobenzene, aniline, aqueous Fe(II), 0.5 N HCl-extractable Fe(II), and pH were quantified as described below.

Abiotic Experiments. The reduction of nitrobenzene by biogenic Fe(II) and by bioreduced NOM was measured in separate experiments (all conducted in deoxygenated 10 mM PIPES, pH 6.8). Hematite (2.0 g L^{-1}) was first bioreduced by CN32 (10^8 cell mL^{-1}) for 3 d to produce 0.18 mM 0.5 N HCl-extractable Fe(II), then the cell−hematite−Fe(II) suspension was pasteurized (85 °C for 1 h). Nitrobenzene was added to the pasteurized suspension at an initial concentration of 13.4 μM and samples were periodically collected over 12 h. NOM (1000 mg L^{-1}) was first bioreduced by CN32 (10^8 cell mL^{-1}) for 2 h (*10, 11*), and the cell-reduced NOM suspension was filter sterilized (0.2 μm). Nitrobenzene was added to the reduced NOM filtrate (940 mg L^{-1}) at an initial concentration of 149 μM, and after 12 h samples were collected to measure nitrobenzene, aniline, and NOM reducing equivalents. Reducing equivalents stored in the NOM, before and after reaction with nitrobenzene, were indirectly measured by the amount of Fe(II) evolved from a 30-min reaction with 5.25 mM ferric citrate (*11*).

Analytical Methods. Nitrobenzene and aniline were measured by an HPLC equipped with a C18 column and photodiode array detector using an acetonitrile/water (1/1 v/v) mobile phase. Aqueous Fe(II) was measured after filtration (0.2 μm) and analyzed using the ferrozine assay. The 0.5 N HCl-extractable Fe(II) was measured after a 24 h extraction, filtered (0.2 μm), and analyzed using the ferrozine assay. Solution pH was measured after filtration using a combination electrode.

Results and Discussion

Bioreduction of Nitrobenzene and NOM. In the absence of NOM, CN32 reduced nitrobenzene stoichiometrically to aniline within 48 h (Figure 2a). No other intermediate products were detected and the total concentration of nitrobenzene plus aniline always exceeded 98.4% of the initial nitrobenzene concentration in both biotic reactors and abiotic controls. The accumulation of aniline effectively demonstrates, as expected, that CN32 cannot use aniline as an electron donor. We believe that this is the first study demonstrating that CN32 can respire on nitrobenzene.

The rate of nitrobenzene reduction by CN32 was observed to be pseudo-first-order with respect to the nitrobenzene concentration (Figure 2b) according to

$$R_{red} = d[\text{nitrobenzene}]/dt = -k_{red} \cdot [\text{nitrobenzene}] \quad (1)$$

where k_{red} is the pseudo-first-order reduction rate constant (h^{-1}). The rate of nitrobenzene reduction can be affected by other factors such as electron donor and its concentration, cell density, temperature, and mixing conditions. Because these factors were the same for all experiments (with the exception of NOM or hematite or lactate addition), they have been excluded from eq 1 for a simplified comparison. In the absence of NOM, k_{red} was 0.085 h^{-1} (Table 1).

Reduction of nitrobenzene was enhanced in the presence of NOM (Figure 2), where k_{red} was 0.58 h^{-1} and 0.16 h^{-1} in the presence of 100 mg L^{-1} SHA and GNOM, respectively. This enhancement effect was dependent on the NOM concentration, where more NOM promoted faster nitrobenzene reduction. Similarly, Borch et al. (*5*) showed that anthraquinone-2,6-disulfonate (AQDS) stimulated the biodegradation of TNT by *Cellulomonas*, and Bhushan et al. (*4*) showed that either AQDS or Aldrich humic acid (1 g L^{-1}) stimulated the biodegradation of RDX by *Clostridium*. However, our results contrast with studies that tested the effect of NOM on the reduction of nitro-compounds. Kwon and Finneran (*1*) showed that the addition of AQDS stimulated the bioreduction of RDX by *G. metallireducens*, but the addition of Aldrich humic acid (250 mg L^{-1}) had little effect. Zhang and Weber (*9*) showed that the addition of juglone stimulated the bioreduction of CNAAzB by CN32, but the addition of Suwannee River natural organic matter (5 mg L^{-1}) had little effect. We speculate our differing results are because nitrobenzene is much more reactive with reduced NOMs as compared to RDX or CNAAzB.

SHA enhanced nitrobenzene reduction significantly more than GNOM ($P < 0.01$), consistent with previous studies which showed that SHA enhanced hematite bioreduction by CN32 more so than GNOM (*12, 13*). Compared to GNOM, SHA has a relatively high aromatic C content and relatively low aliphatic, alcoholic, and carbohydrate C content (*12, 19*). SHA also contains a higher organic radical content (12.9 × 10^{17} spins g^{-1}) as compared to GNOM (6.67 × 10^{17} spins g^{-1}) (*12*) that presumably reflects a higher quantity of quinone moieties capable of participating in electron transfer reactions (*11*).

Abiotic Reduction of Nitrobenzene by Bioreduced NOM. Reducing equivalents stored in bioreduced, filter-sterilized SHA and GNOM were indirectly measured by reaction with ferric citrate (*11*). The reducing equivalents stored in bioreduced SHA was 0.32 eq kg^{-1}, nearly equal to the value of 0.34 eq kg^{-1} reported by Scott et al. (*11*), and an order of magnitude higher than measured for GNOM (0.034 eq kg^{-1}) (Supporting

TABLE 1. Summary of Pseudo-First-Order Rate Constants (Mean ± SD) for Nitrobenzene Reduction with Combinations of *Shewanella putrefaciens* CN32, Natural Organic Matter (NOM), and Hematite

reaction no. in Figure *1*	reaction description	experimental components					first-order kinetics		
		CN32[a]	nitrobenzene (μM)	NOM (mg L^{-1})	hematite (g L^{-1})	electron donor[b]	time (h)	k_{red} (h^{-1})	R^2
R_1	nitrobenzene bioreduction	+	149	0	0	H_2	0−10	0.085 ± 0.0027	0.996
R_1	nitrobenzene bioreduction	+	1,490	0	0	H_2	0−4	0.036 ± 0.0018	0.998
							4−10	0.0029 ± 0.0003	0.985
R_1	nitrobenzene bioreduction	+	1,490	0	0	H_2 and lactate	0−4	0.043 ± 0.0021	0.998
							4−96	0.0058 ± 0.0002	0.994
R_4	nitrobenzene reduction by Fe(II)-Fe_2O_3	−	13.4	0	2.0	Fe(II)[c]	0−1	0.14	1.00
							1−12	0.035 ± 0.0017	0.989
R_1 and $R_2 + R_4$	nitrobenzene reduction with hematite	+	149	0	2.0	H_2	0−10	0.13 ± 0.0032	0.998
R_1 and $R_2 + R_4$	nitrobenzene reduction with hematite	+	149	0	0.2	H_2	0−10	0.097 ± 0.0024	0.998
R_1 and $R_2 + R_4$	nitrobenzene reduction with hematite	+	1,490	0	2.0	H_2	0−4	0.035 ± 0.0038	0.989
							4−10	0.0029 ± 0.0003	0.985
R_1 and $R_2 + R_4$	nitrobenzene reduction with hematite	+	1,490	0	2.0	H_2 and lactate	0−4	0.050 ± 0.0105	0.956
							4−96	0.0071 ± 0.0003	0.990
R_1 and $R_3 + R_5$	nitrobenzene reduction with NOM	+	149	100 SHA	0	H_2	0−6	0.59 ± 0.053	0.967
R_1 and $R_3 + R_5$	nitrobenzene reduction with NOM	+	149	10 SHA	0	H_2	0−10	0.16 ± 0.0023	0.999
R_1 and $R_3 + R_5$	nitrobenzene reduction with NOM	+	149	100 GNOM	0	H_2	0−10	0.16 ± 0.0027	0.998
R_1 and $R_3 + R_5$	nitrobenzene reduction with NOM	+	149	10 GNOM	0	H_2	0−10	0.11 ± 0.0048	0.992
R_1 and $R_2 + R_4$ and $R_3 + R_5$ and $R_3 + R_6 + R_4$	nitrobenzene reduction with hematite and NOM	+	149	100 SHA	2.0	H_2	0−6	0.53 ± 0.0537	0.961
R_1 and $R_2 + R_4$ and $R_3 + R_5$ and $R_3 + R_6 + R_4$	nitrobenzene reduction with hematite and NOM	+	149	100 GNOM	2.0	H_2	0−10	0.23 ± 0.0069	0.995

[a] 1×10^8 cells mL^{-1} (+) or 0 (−). [b] H_2 = 2.5% H_2 in 60 mL headspace over 100 mL fluid; lactate = 5 mM. [c] 0.18 mM 0.5 N HCl-extractable Fe(II).

TABLE 2. Summary of Zero-Order Rates for Electron Transfer Reactions with Combinations of *Shewanella putrefaciens* CN32, Natural Organic Matter (NOM), and Hematite

reaction no. in Figure *1*	reaction description	experimental components					zero-order kinetics	
		CN32[a]	nitrobenzene (μM)	NOM (mg L^{-1})	hematite (g L^{-1})	electron donor[b]	time (h)	rate (μeq L^{-1} h^{-1})
R_1	nitrobenzene bioreduction	+	149	0	0	H_2	0−10	52.9
R_2	hematite bioreduction	+	0	0	2.0	H_2	0−10	6.87
R_3	NOM bioreduction	+	0	1,000 SHA	0	H_2	0−2	122
R_3	NOM bioreduction	+	0	1,000 GNOM	0	H_2	0−2	16.2
R_4	nitrobenzene reduction by Fe(II)−Fe_2O_3	−	13.4	0	2.0	Fe(II)[c]	0−9	2.58
R_5	nitrobenzene reduction by NOM	−	149	940 SHA	0	reduced SHA	0−12	8.50
R_5	nitrobenzene reduction by NOM	−	149	940 GNOM	0	reduced GNOM	0−12	0.0
R_6	Fe(III) reduction by NOM	−		940 SHA	[d]	reduced SHA	0−0.5	594
R_6	Fe(III) reduction by NOM	−		940 GNOM	[d]	reduced GNOM	0−0.5	64.8

[a] 1×10^8 cells mL^{-1} (+) or 0 (−). [b] H_2 = 2.5% H_2 in 60 mL headspace over 100 mL fluid. [c] 0.18 mM 0.5 N HCl-extractable Fe(II). [d] Measurements conducted with 5.25 mM ferric citrate, NOT hematite.

Information Figure S1). Unaltered (not bioreduced by CN32) SHA contained some reducing equivalents (0.048 eq kg^{-1}) while unaltered GNOM contained none. In abiotic experiments, bioreduced SHA was capable of reducing a portion of the nitrobenzene while bioreduced GNOM was not. While these experiments were conducted with a large excess of nitrobenzene (149 μM = 894 μeq electrons L^{-1}) relative to bioreduced NOM (297 and 32 μeq L^{-1} with SHA and GNOM, respectively), the bioreduced NOMs were still able to reduce ferric citrate added at the conclusion of the nitrobenzene reduction period. Our interpretation of this result is that a fraction of the redox active moieties in bioreduced NOM had reduction potentials less than the reduction potential of nitrobenzene.

Evaluation of Electron Flow to Nitrobenzene in the Presence of NOM. Based on our conceptualization of the operative redox reactions in these systems (Figure 1), the presence of NOM could enhance nitrobenzene reduction by serving as a preferred electron acceptor (R_3) and facile electron shuttle (R_5). To quantify electron flow in our experiments we calculated zero-order reaction rates in terms of electron equivalents transferred L^{-1} h^{-1} (Table 2). Zero-order rates were used because in several abiotic experiments sampling frequency was not high enough to fit any other rate law.

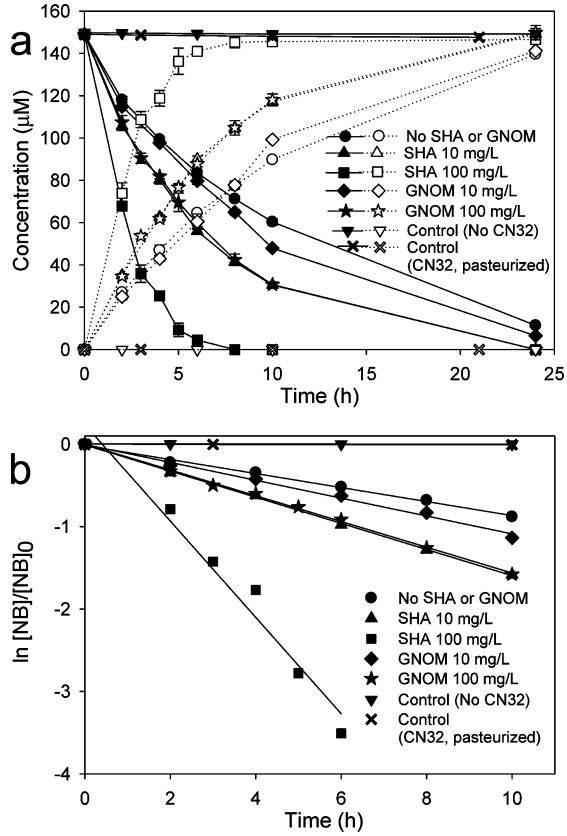

FIGURE 2. Biological reduction of nitrobenzene by *Shewanella putrefaciens* CN32 (1.0×10^8 cells mL^{-1}) in the absence and presence of soil humic acid (SHA) and Georgetown natural organic matter (GNOM). Experiments were conducted with 149 μM nitrobenzene and H_2 (2.5% headspace) in 10 mM PIPES, pH 6.8. (a) Nitrobenzene (solid symbols) and aniline (open symbols) concentrations as a function of incubation time. Control contained 100 mg L^{-1} humic acid and no CN32. Symbols represent means of triplicate measurements and error bars represent 1 standard deviation. (b) Nitrobenzene concentrations transformed to Ln($[C_t]/[C_0]$) to calculate pseudo-first-order reduction rates.

Based on these comparisons, we found that CN32 could transfer electrons from H_2 to SHA faster (122 μeq L^{-1} h^{-1}) than it could transfer electrons to nitrobenzene (52.9 μeq L^{-1} h^{-1}). Reduced SHA could then transfer electrons to nitrobenzene, although our calculated rate of 8.5 μeq L^{-1} h^{-1} for this reaction could be significantly underestimated because it was based on a single measurement after 12 h. Reduced GNOM appeared incapable of abiotic reduction of nitrobenzene yet enhanced bioreduction of nitrobenzene. One possible explanation of the GNOM results is that GNOM can function as an electron shuttle only in the presence of a continuous source of electron as provided by CN32. The GNOM results highlight shortcomings of "component experiments" (e.g., isolation of R5) where the reactivity of one component (i.e., GNOM) contrasts with its reactivity in a multicomponent system (i.e., CN32 plus GNOM).

When SHA was increased from 10 to 100 mg L^{-1}, electron flow from H_2 through SHA (via CN32) to nitrobenzene increased. Under these conditions we suggest that NOM-mediated nitrobenzene reduction ($R_3 + R_5$) became the predominant reaction mechanism. Furthermore, we propose that electron transfer from reduced NOM to nitrobenzene (R_5) was the rate-limiting step in this coupled process. At the lower SHA concentration (10 mg L^{-1} = 5.8 mg C L^{-1}), more relevant to natural terrestrial systems, we believe electron flow via direct nitrobenzene bioreduction (R_1) was still important.

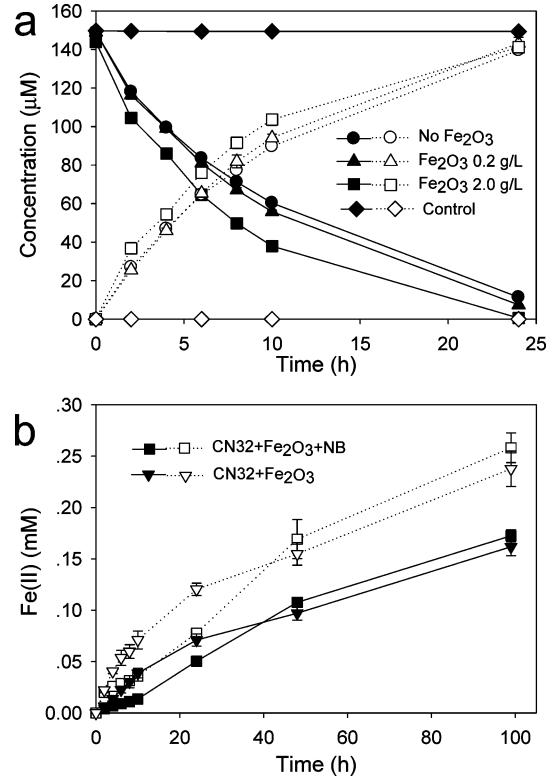

FIGURE 3. Biological reduction of nitrobenzene by *Shewanella putrefaciens* CN32 (1.0×10^8 cells mL^{-1}) in the absence and presence of hematite (Fe_2O_3). Experiments were conducted with 149 μM nitrobenzene and H_2 (2.5% headspace) in 10 mM PIPES, pH 6.8. (a) Nitrobenzene (solid symbols) and aniline (open symbols) concentrations over first 24 h. Control contained 2.0 g L^{-1} Fe_2O_3 and no CN32. Symbols represent means of triplicate measurements and error bars represent 1 standard deviation. (b) 0.5 N HCl-extractable Fe(II) (open symbols) and aqueous Fe(II) (solid symbols) concentrations with 2.0 g L^{-1} Fe_2O_3 over first 100 h.

Bioreduction of Nitrobenzene and Hematite. Hematite was chosen for this study because it is resistant to phase transformations during bioreduction which simplifies data interpretation. In addition, reactions between Fe(II) and hematite have been well characterized with respect to the possible types of reactive Fe(II) species (*20*−*22*). In the following discussion we refer to "solid-associated Fe(II)" as Fe(II) adsorbed to the hematite surface or formed within the solid due to electrons being transposed into the bulk crystal lattice (*23, 24*). Solid-associated Fe(II) was operationally defined as the difference between the 0.5 N HCl-extractable and aqueous Fe(II) concentrations.

The kinetics of nitrobenzene bioreduction were enhanced in the presence of hematite (Figure 3a), where k_{red} was 0.097 h^{-1} and 0.13 h^{-1} in the presence of 0.2 and 2.0 g L^{-1} hematite, respectively (Table 1). Compared to hematite controls prepared with no nitrobenzene, Fe(II) production in the first 24 h was significantly less ($P < 0.01$) in the presence of nitrobenzene (Figure 3b). A net decrease in Fe(II) production was likely caused by the abiotic reduction of nitrobenzene thereby consuming biogenic-Fe(II). Because CN32 could transfer electrons from H_2 to nitrobenzene faster (52.9 μeq L^{-1} h^{-1}) than it could transfer electrons to hematite (6.9 μeq L^{-1} h^{-1}), Fe(II)-mediated nitrobenzene reduction ($R_2 + R_4$ in Figure 1) was not as important in this experimental system as compared to how important NOM-mediated nitrobenzene reduction ($R_3 + R_5$) was in the NOM-amended experimental systems.

The enhancement of nitrobenzene reduction by hematite was dependent on the presence of excess electron donor.

With 149 μM nitrobenzene, H_2 in the reactors did not limit the extent of nitrobenzene bioreduction (Figure 3). However, in identical experiments conducted with 1490 μM nitrobenzene, bioreduction was incomplete with the same H_2 headspace concentration (Supporting Information Figure S2). With the inclusion of 5 mM lactate, CN32 was able to completely reduce this higher concentration of nitrobenzene. Under electron donor-limiting conditions (1490 μM nitrobenzene with H_2), nitrobenzene reduction was not enhanced by hematite but instead was slightly inhibited. Under conditions with excess electron donor (149 μM nitrobenzene with H_2—Figure 3; 1490 μM nitrobenzene with H_2 and lactate—Figure S2), hematite always enhanced nitrobenzene reduction. Our interpretation of these results is that nitrobenzene bioreduction (R_1) and hematite bioreduction (R_2) became competitive processes under electron donor-limiting conditions. So while reducing equivalents were transferred/diverted to hematite, all of those electrons were not ultimately transferred to nitrobenzene (R_4).

Abiotic Reduction of Nitrobenzene by Fe(II)−Hematite. In experiments conducted with pasteurized cell−hematite−biogenic-Fe(II) suspensions, nitrobenzene was reduced to aniline in stoichiometric agreement with total Fe(II) consumption (Figure 4c). Both aqueous and solid-associated Fe(II) were consumed in this reaction (Figure 4b). The abiotic reduction kinetics of nitrobenzene (R_4) displayed biphasic behavior where a brief period (0−1 h) of relatively fast reduction ($k_{red} = 0.14\ h^{-1}$) was followed by a longer period (1−12 h) of slow reduction ($k_{red} = 0.035\ h^{-1}$) (Figure 4a).

We believe these results are consistent with an evolving conceptual model for heterogeneous oxidation of Fe(II) at the surface of Fe(III) oxides (*20, 21, 23−25*). The solid-associated form of Fe(II) is presumably the most reactive species (thus kinetically favored) yet aqueous Fe(II) is required for contaminant reduction to occur (*21, 23*). Furthermore, because hematite is a semiconductive solid, electrons accepted by surface-associated Fe(II) at one location could be transferred through the bulk crystal to another location (*24*). Therefore, it is possible that the dynamics between aqueous, sorbed, and structural Fe(II), and the corresponding current flow through the bulk crystal, may account for the biphasic behavior of nitrobenzene reduction observed in our experiments.

Based on these experiments, the zero-order rate of electron transfer from hematite−Fe(II) to nitrobenzene (R_4) was 8.50 μeq L^{-1} h^{-1} (Table 2), higher than the CN32-mediated rate of electron transfer to hematite (R_2; 6.9 μeq L^{-1} h^{-1}). The rate of hematite bioreduction has been shown to be proportional to the oxide concentration (*26, 27*), such that the rate of R_2 should have increased when the hematite concentration was increased from 0.2 to 2.0 g L^{-1}. This did indeed occur in our experiments (Figure 3b). From these results we conclude that the rate of hematite bioreduction was the rate-limiting step in the indirect Fe(II)-mediated reduction of nitrobenzene ($R_2 + R_4$). However, we still believe that direct bioreduction of nitrobenzene (R_1) was the predominant removal mechanism in this experimental system.

Bioreduction of Nitrobenzene, NOM, and Hematite. The combined effects of NOM and hematite also increased the reduction kinetics of nitrobenzene (Figure 5a). Using the same nitrobenzene, H_2, and cell concentrations, k_{red} increased from 0.085 h^{-1} (no NOM, no Fe_2O_3) to 0.58 h^{-1} (100 mg L^{-1} SHA, no Fe_2O_3) to 0.13 h^{-1} (no NOM, 2.0 g L^{-1} Fe_2O_3) to 0.53 h^{-1} (100 mg L^{-1} SHA, 2.0 g L^{-1} Fe_2O_3). With GNOM, k_{red} increased to 0.16 h^{-1} (100 mg L^{-1} GNOM, no Fe_2O_3) and to 0.23 h^{-1} (100 mg L^{-1} GNOM, 2.0 g L^{-1} Fe_2O_3). These results demonstrate, not surprisingly, that different NOMs behave differently in these multicomponent experimental systems.

An overarching goal of this research was to better understand electron flow that leads to contaminant reduction in systems containing NACs, DMRB, Fe(III) solids, and NOM.

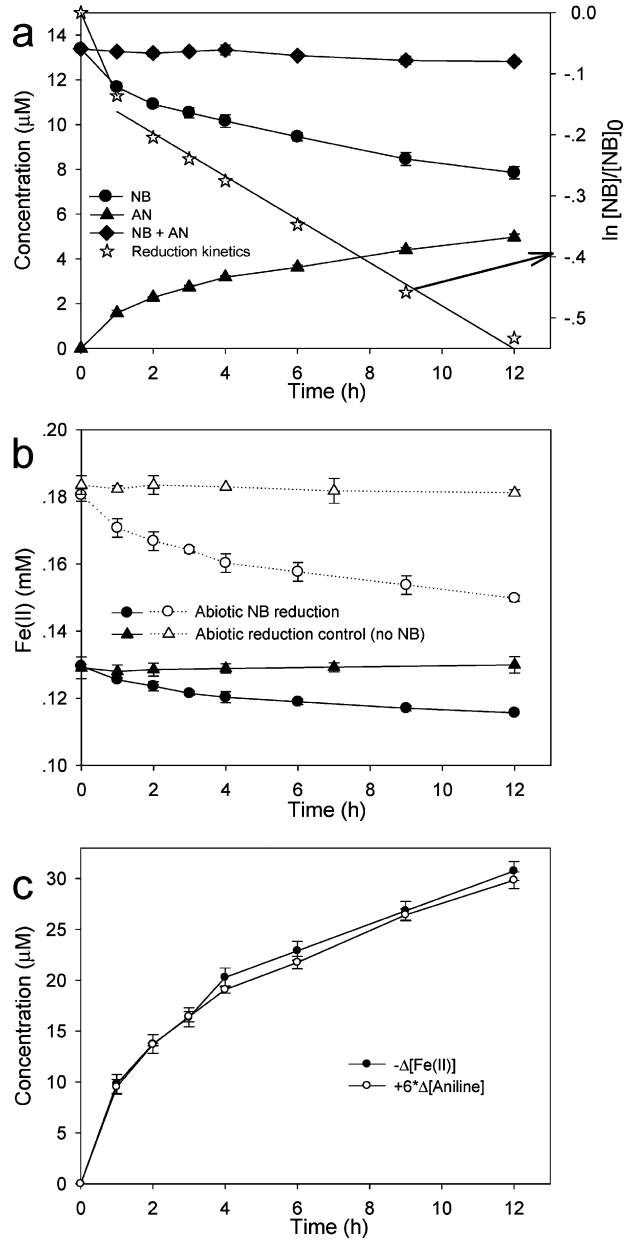

FIGURE 4. Abiotic reduction of nitrobenzene by pasteurized cell−hematite−biogenic Fe(II) suspensions. Experiments were conducted with 13.4 μM nitrobenzene and 0.18 mM 0.5 N HCl-extractable Fe(II) produced from 2.0 g L^{-1} Fe_2O_3 and 1.0 × 10^8 cells mL^{-1} *S. putrefaciens* CN32 in 10 mM PIPES, pH 6.8. (a) Nitrobenzene and aniline concentrations as a function of reaction time. Nitrobenzene concentrations manipulated (open stars) to calculate pseudo-first-order reduction rate. (b) 0.5 N HCl-extractable Fe(II) (open symbols) and aqueous Fe(II) (solid symbols) concentrations as a function of reaction time. Control contained no nitrobenzene. (c) Concomitant production of aniline and consumption of Fe(II) demonstrating stoichiometric relationship. The aniline concentration is multiplied by six because six electrons are transferred in the reduction of nitrobenzene to aniline.

The challenge then was to rank the importance of the four parallel reaction paths envisioned that lead to nitrobenzene reduction (a−d in Figure 1). We propose that NOM-mediated reduction of nitrobenzene ($R_3 + R_5$) was the most important mechanism in our experimental system. First, based on the competitive utilization of available electron acceptors, we found that CN32 reduced SHA faster (122 μeq L^{-1} h^{-1}) than nitrobenzene (52.9 μeq L^{-1} h^{-1}) or hematite (6.9 μeq L^{-1} h^{-1}).

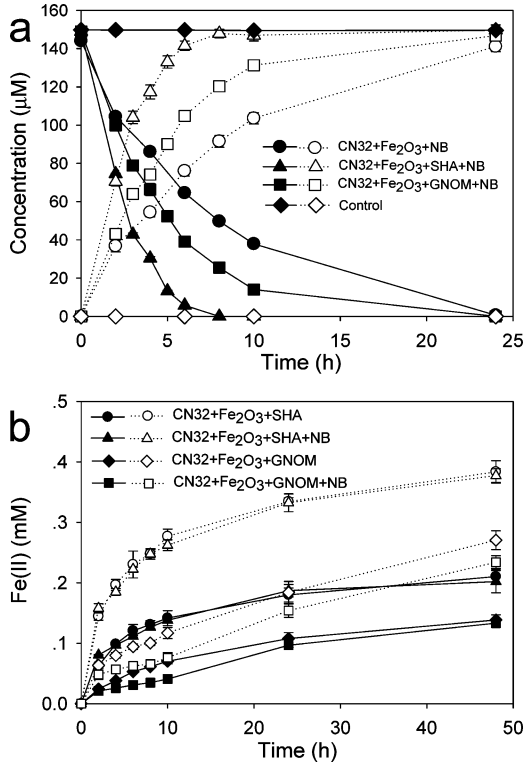

FIGURE 5. Biological reduction of nitrobenzene and hematite (Fe_2O_3) by *Shewanella putrefaciens* CN32 (1.0×10^8 cells mL^{-1}) in the absence and presence of soil humic acid (SHA) and Georgetown natural organic matter (GNOM). Experiments were conducted with 149 μM nitrobenzene, H_2 (2.5% headspace), 2.0 g L^{-1} Fe_2O_3, and 0 or 100 mg L^{-1} SHA or GNOM in 10 mM PIPES, pH 6.8. (a) Nitrobenzene (solid symbols) and aniline (open symbols) concentrations over first 24 h. Control contained 2.0 g L^{-1} Fe_2O_3, 100 mg L^{-1} SHA, and no CN32. (b) 0.5 N HCl-extractable Fe(II) (open symbols) and aqueous Fe(II) (solid symbols) concentrations over first 48 h. Symbols represent means of triplicate measurements and error bars represent 1 standard deviation.

This claim is consistent with Jiang and Kappler (*14*) who reported that *G. sulfurreducens* reduced IHSS humic substances at least 27 times faster than it reduced ferrihydrite. Bioreduced NOM could then transfer electrons to nitrobenzene (R_5) or to hematite (R_6) and be reoxidized to continue its catalytic function. Based on the rate and extent of hematite bioreduction measured with 0 (Figure 3b) or 100 mg L^{-1} GNOM (Figure 5b), Fe(II) production was not significantly enhanced ($P < 0.01$), yet the rate of nitrobenzene reduction significantly increased ($P < 0.01$) from 0.085 to 0.23 h^{-1}. Our interpretation of this result is that electrons from reduced GNOM were preferentially transferred to nitrobenzene versus hematite, such that the coupled reaction path of $R_3 + R_5$ was faster than the coupled reaction path of $R_3 + R_6 + R_4$ (Figure 1). A contributing factor to this could be that NOM inhibited hematite−Fe(II) reduction of nitrobenzene (R_4) as observed in studies on abiotic reactions between nitro-compounds, Fe(II), Fe(III) solids, and NOM (*15, 16*).

Another line of evidence supporting the importance of NOM-mediated reduction of nitrobenzene can be inferred from the results obtained with SHA. With 100 mg L^{-1} SHA, the addition of hematite decreased the rate of nitrobenzene reduction from 0.58 h^{-1} (Figure 2a—no hematite) to 0.53 h^{-1} (Figure 5a—2.0 g L^{-1} hematite). This decrease in the rate of nitrobenzene reduction occurred even in the presence of the highest Fe(II) concentrations measured in these experiments (Figure 5b). Our interpretation of these data is that while reduced SHA effectively transferred electrons to hematite, hematite−Fe(II) displayed limited reactivity toward nitrobenzene in the presence of SHA. Our conclusion that NOM-mediated reduction of nitrobenzene was the predominant mechanism agrees and contrasts with related studies. Hofstetter et al. (*7*) concluded that TNT reduction by solid-associated Fe(II) was more important than by reduced quinones, while Zhang and Weber (*9*) concluded that CNAAzB reduction occurred through a solution phase pathway via reduced NOM, and Kwon and Finneran (*3*) concluded that RDX reduction occurred concurrently by both solid-associated Fe(II) and reduced quinones. Differing conclusions drawn from these studies highlight the difficulty in generalizing contaminant behavior in increasingly complex systems but also highlight the need for additional research in this area.

Acknowledgments

Funding for F.L. was provided through the China Scholarship Council. Support for W.B. was provided by the National Science Foundation under Grant CHE-0431328.

Supporting Information Available

Abiotic reactions between bioreduced, filter-sterilized NOM solutions and nitrobenzene or Fe(III)citrate; and, biological reduction of nitrobenzene and hematite in the absence and presence of excess electron donor. This material is available free of charge via the Internet at http://pubs.acs.org.

Literature Cited

(1) Kwon, M. J.; Finneran, K. T. Microbially mediated biodegradation of hexahydro-1,3,5-trinitro-1,3,5-triazine by extracellular electron shuttling compounds. *Appl. Environ. Microbiol.* **2006**, *72*, 5293–5941.

(2) Kwon, M. J.; Finneran, K. T. Hexahydro-1,3,5-trinitro-1,3,5-triazine (RDX) and octahydro-1,3,5,7-tetranitro-1,3,5,7-tetrazocine (HMX) biodegradation kinetics amongst several Fe(III)-reducing genera. *Soil Sed. Contam.* **2008**, *17*, 189–203.

(3) Kwon, M. J.; Finneran, K. T. Hexahydro-1,3,5-trinitro-1,3,5-triazine (RDX) reduction is concurrently mediated by direct electron transfer from hydroquinones and resulting biogenic Fe(II) formed during electron shuttle-amended biodegradation. *Environ. Eng. Sci.* **2009**, *26*, 961–971.

(4) Bhushan, B.; Halasz, A.; Hawari, J. Effect of iron(III), humic acids and anthraquinone-2,6-disulfonate on biodegradation of cyclic nitramines by *Clostridium* sp. EDB2. *J. Appl. Microbiol.* **2006**, *100*, 555–563.

(5) Borch, T.; Inskeep, W. P.; Harwood, J. A.; Gerlach, R. Impact of ferrihydrite and anthraquinone-2,6-disulfonate on the reductive transformation of 2,4,6-trinitrotoluene by a gram-positive fermenting bacterium. *Environ. Sci. Technol.* **2005**, *39*, 7126–7133.

(6) Heijman, C. G.; Holliger, C.; Glaus, M. A.; Schwarzenbach, R. P.; Zeyer, J. Abiotic reduction of 4-chloronitrobenzene to 4-chloroaniline in a dissimilatory iron-reducing enrichment culture. *Appl. Environ. Microbiol.* **1993**, *59*, 4350–4353.

(7) Hofstetter, T. B.; Heijman, C. G.; Haderlein, S. B.; Holliger, C.; Schwarzenbach, R. P. Complete reduction of TNT and other (poly)nitroaromatic compounds under iron reducing subsurface conditions. *Environ. Sci. Technol.* **1999**, *33*, 1479–1487.

(8) Tobler, N. B.; Hofstetter, T. B.; Straub, K. L.; Fontana, D.; Schwarzenbach, R. P. Iron-mediated microbial oxidation and abiotic reduction of organic contaminants under anoxic conditions. *Environ. Sci. Technol.* **2007**, *41*, 7765–7772.

(9) Zhang, H. C.; Weber, E. J. Elucidating the role of electron shuttles in reductive transformations in anaerobic sediments. *Environ. Sci. Technol.* **2009**, *43*, 1042–1048.

(10) Lovley, D. R.; Coates, J. D.; Blunt-Harris, E. L.; Phillips, E. J. P.; Woodward, J. C. Humic substances as electron acceptors for microbial respiration. *Nature* **1996**, *382*, 445–448.

(11) Scott, D. T.; McKnight, D. M.; Blunt-Harris, E. L.; Kolesar, S. E.; Lovley, D. R. Quinone moieties act as electron acceptors in the reduction of humic substances by humics-reducing microorganisms. *Environ. Sci. Technol.* **1998**, *32*, 2984–2989.

(12) Royer, R. A.; Burgos, W. D.; Fisher, A. S.; Jeon, B. H.; Unz, R. F.; Dempsey, B. A. Enhancement of hematite bioreduction by

natural organic matter. *Environ. Sci. Technol.* **2002**, *36*, 2897–2904.
(13) Chen, J.; Gu, B. H.; Royer, R. A.; Burgos, W. D. The roles of natural organic matter in chemical and microbial reduction of ferric iron. *Sci. Total Environ.* **2003**, *307*, 167–178.
(14) Jiang, J.; Kappler, A. Kinetics of microbial and chemical reduction of humic substances: Implications for electron shuttling. *Environ. Sci. Technol.* **2008**, *42*, 3563–3569.
(15) Colon, D.; Weber, E. J.; Anderson, J. L. QSAR study of the reduction of nitroaromatics by Fe(II) species. *Environ. Sci. Technol.* **2006**, *40*, 4976–4982.
(16) Hakala, J. A.; Chin, Y.-P.; Weber, E. J. Influence of dissolved organic matter and Fe(II) on the abiotic reduction of pentachloronitrobenzene. *Environ. Sci. Technol.* **2007**, *41*, 7337–7342.
(17) Senko, J. M.; Kelly, S. D.; Dohnalkova, A. C.; McDonough, J. T.; Kemner, K. M.; Burgos, W. D. The effect of U(VI) bioreduction kinetics on subsequent reoxidation of UO_2. *Geochim. Cosmochim. Acta* **2007**, *71*, 4644–4654.
(18) Gu, B. H.; Schmitt, J.; Chen, Z. H.; Liang, L. Y.; McCarthy, J. F. Adsorption and desorption of natural organic-matter on iron-oxide - mechanisms and models. *Environ. Sci. Technol.* **1994**, *28*, 38–46.
(19) Thorn, K. A.; Folan, D. W.; MacCarthy, P. *Characterization of the International Humic Substances Society standard and reference fulvic and humic acids by solution state carbon-13 and hydrogen-1 nuclear magnetic resonance spectroscopy*; U.S. Geological Survey, 1989.
(20) Jeon, B.-H.; Dempsey, B. A.; Burgos, W. D. Kinetics and mechanisms for reactions of Fe(II) with iron(III) oxides. *Environ. Sci. Technol.* **2003**, *37*, 3309–3315.
(21) Williams, A. B.; Scherer, M. M. Spectroscopic evidence for Fe(II)-Fe(III) electron transfer at the iron oxide-water interface. *Environ. Sci. Technol.* **2004**, *38*, 4782–4790.
(22) Jang, J. H.; Dempsey, B. A.; Burgos, W. D. Solubility of hematite revisited: Effects of hydration. *Environ. Sci. Technol.* **2007**, *41*, 7303–7308.
(23) Park, B.-T.; Dempsey, B. A. Heterogeneous oxidation of Fe(II) on ferric oxide at neutral pH and a low partial pressure of O_2. *Environ. Sci. Technol.* **2005**, *39*, 6494–6500.
(24) Yanina, S. V.; Rosso, K. M. Linked reactivity at mineral-water interfaces through bulk crystal conduction. *Science* **2008**, *320*, 218–222.
(25) Handler, R. M.; Beard, B. L.; Johnson, C. M.; Scherer, M. M. Atom Exchange between Aqueous Fe(II) and Goethite: An Fe Isotope Tracer Study. *Environ. Sci. Technol.* **2009**, *43*, 1102–1107.
(26) Burgos, W. D.; Fang, Y. L.; Royer, R. A.; Yeh, G. T.; Stone, J. J.; Jeon, B.-H.; Dempsey, B. A. Reaction-based modeling of quinone-mediated bacterial iron(III) reduction. *Geochim. Cosmochim. Acta* **2003**, *67*, 2735–2748.
(27) Roden, E. E.; Zachara, J. M. Microbial reduction of crystalline iron(III) oxides: Influence of oxide surface area and potential for cell growth. *Environ. Sci. Technol.* **1996**, *30*, 1618–1628.

ES901585Z